

Bistability between different dissipative solitons in nonlinear optics

U. Bortolozzo, L. Pastur, P.L. Ramazza

Istituto Nazionale di Ottica Applicata, Largo E. Fermi 6, I50125 Florence, Italy

M. Tlidi

*Optique Nonlinéaire Théorique, Université Libre de Bruxelles,
CP 231, Campus Plaine, 1050 Bruxelles, Belgium*

G. Kozyreff

Mathematical Institute, 24-29 St Giles', Oxford OX1 3LB, United Kingdom

(Dated: November 20, 2018)

We report the observation of different localized structures coexisting for the same parameter values in an extended system. The experimental findings are carried out in a nonlinear optical interferometer, and are fully confirmed by numerical simulations. The existence of each kind of localized structure is put in relation to a corresponding delocalized pattern observed. Quantitative evaluation of the range of pump parameter allowing bistability between localized structures is given. The dependence of the phenomena on the other relevant parameters is discussed.

PACS: 05.45.Yv,42.65.Sf,42.65.Tg,47.54.+r

Localization of structures is a widespread phenomenon occurring both in conservative and in dissipative systems. The study of this topic aims on the one hand to an understanding of the general conditions needed for the occurrence of localized structures (LS); and, on the other hand, to explore the potentialities offered by these objects in view of applications, such as information transmission and storage. In this context, LS have been demonstrated in many diverse fields, including granular materials [1], fluid dynamics [2], electroconvection in liquid crystals [3], chemistry [4] and nonlinear optics [5].

With specific reference to optical systems, temporal solitons represent a classic and very active field of research. Recently, spatial localized structures in extended nonlinear optical system have been widely studied as well [5].

An important class of spatial LS, often referred to as cavity solitons, exists in many dissipative optical systems [6]. These solitons can be used as pixels for information storage or processing [7, 8]. Their existence has been experimentally demonstrated in several devices [9, 10, 11, 12, 13], including miniaturized semiconductor resonators [12, 13].

In this paper we present the experimental evidence of bistability between different localized structures in a dissipative nonlinear optical device. The two kind of solitons we find differ in shape, and are separated by a discrete gap in their peak intensity. If used as pixels for information storage, these LS represent three-state variables, instead of the common two-state variables ("bits") that a common soliton can encode. Consequently, use of these new solitons would lead to an increase of $\log_2 3 \simeq 1.585$ for the information storable in a given area.

Localized structure bistability is observed in the presence of two modulational instabilities having different

critical wavenumbers. The question of the interaction between these two instabilities has been investigated in [16] for semiconductor cavities.

The existence of bistable solitons has been predicted in the context of modified nonlinear Schroedinger equations[14, 15], describing light propagation in conservative systems (e.g., optical fibers in the ideal, lossless case). For the spatial dissipative solitons, multistability behaviour of either single or multi-peaked structures has been predicted numerically in nonlinear optical resonators [7, 17, 18]. To our knowledge, an experimental observation of bistability between different LS has not yet been given, neither in optics nor in other fields.

Our experimental system is a nonlinear interferometer formed by a Liquid Crystal Light Valve (LCLV) with optical feedback. The phase φ of an initially plane laser beam sent onto the device evolves as [19]

$$\tau \frac{\partial \varphi}{\partial t} = -(\varphi - \varphi_0) + l_d^2 \nabla_{\perp}^2 \varphi + f(I_{fb}) \quad (1)$$

$$I_{fb} = I_0 | e^{i l_d \nabla_{\perp}^2 / 2k_0} (B e^{i\varphi} + 1 - B) * \text{sinc}(\vec{q}_B \cdot \vec{r}) |^2 \quad (2)$$

$$f(I_{fb}) = \varphi_{sat} (1 - e^{-\frac{I_{fb}}{\varphi_{sat}}}) \quad (3)$$

where l_d is the diffusion length of the LCLV, I_{fb} the feedback intensity on the valve, and φ_0 the phase retardation induced by the valve on the input beam in the absence of feedback. In (2), I_0 is the input intensity, B and $1 - B$ are the fractions of the field along the principal directions of polarization of the cavity, $\text{sinc}(\vec{q}_B \cdot \vec{r})$ represent the spatial filtering and $*$ denotes a convolution product.

The parameters φ_{sat} , τ and α represent respectively the saturation phase value, the response time and the sensitivity of the LCLV. Finally, l is the propagation distance inside the optical loop.

Eq. (3) describes the LCLV nonlinearity. In several circumstances, the phenomena observed in this system can be understood by expanding the exponential term in (3) to the first order, so that a Kerr approximation is obtained [11]. For the topics of interest here, it is instead important to take into account the saturating character of the nonlinearity.

It is well known that this system displays an extremely rich set of different dynamical behaviours [10, 11, 20, 21, 22, 23], and that extended as well as localized patterns can be formed in the transverse wavefront of the beam sent to the interferometer. For the present study, we set the system parameters at $l = 30$ mm, $l_d \simeq 18$ μ m, $B \simeq 0.52$, $\varphi_{sat} = 5$, $\varphi_0 = 0$ and the spatial bandwidth $q_B = 3.7$. Here and in the following, the spatial frequencies are expressed in units of the diffractive scale $q_{diff} = 2\pi/\sqrt{2\lambda}l$, where λ is the optical wavelength.

In our system, one type of LS has been shown to exist over very broad ranges of parameters [10, 11, 25]. It has circular symmetry, with a bright central peak connected to the dark background via a series of small amplitude oscillations along the radial direction. Here, we report another completely different localized solution exists for the same device. The two solitons, as observed in the experiment, are shown in Fig. 1. Numerical simulations faithfully reproduce the observations.

The most evident feature of the new LS is its triangular symmetry, observed both in the central peak and in the tails. Hence, in the following we refer to these structures as Triangular Solitons (TS), and to the ones with circular symmetry as round LS.

A second fundamental difference between triangular and round LS is their peak intensity. This can be appreciated in Fig. 1c, 1d. Finally the size of the central peak is substantially smaller for a TS than for a round LS, though the overall size of the two structures including the tails are comparable.

The triangular soliton and the round LS shown in Fig. 1 are observed for identical values of all the parameters, indicating bistability between the two structures.

The existence of solitons with triangular symmetry has been predicted recently reported in optical systems [26]. However, no bistability between RS and TS is observed in these systems.

Each of these solitons can be switched on by an appropriate addressing pulse. Lower intensity pulses trigger a round LS, higher intensity ones a TS. In these regards, the observed weak sensitivity to the addressing intensity suggests the existence of large basins of attraction for each soliton; hence, the noise is not expected to be a serious limit in the use of these structures for information storage and processing tasks.

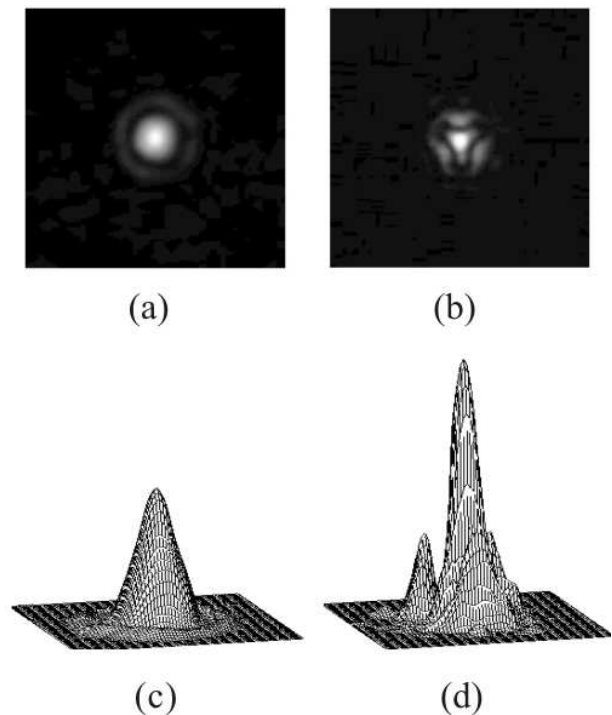


FIG. 1: (a), (c): Round soliton; (b), (d): Triangular soliton.

We are now going to investigate the dependence of the phenomena observed on the pump intensity. The experimental state diagram of the system is shown in Fig. 2.

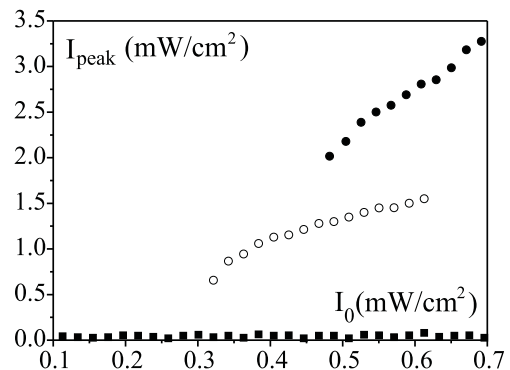


FIG. 2: Experimental state diagram of the system. Squares: low uniform state; empty circles: round localized structures; filled circles: triangular solitons.

Starting from a very low value of input intensity and gradually increasing it, the lower uniform solution is the only state observed up to $I_0 \simeq 0.32$. From this value on, round LS are observable, when addressed via proper initial conditions. At $I_0 \simeq 0.61$ mW/cm^2 the round LS loses its stability, and the system jumps to the triangular solitons branch. If, starting from a TS, the pump is decreased, the structure remains stable down to $I_0 \simeq 0.47$

mW/cm^2 , and then decays to a round LS. If, instead, starting from $I_0 \simeq 0.61 mW/cm^2$, the pump is increased, the TS exists up to $I_0 \simeq 0.69 mW/cm^2$, and then destabilizes via a transition to a delocalized irregular pattern.

The range of bistability between different LS is therefore $0.47 \lesssim I_0 \lesssim 0.61 mW/cm^2$. Above $\simeq 2 mW/cm^2$ the system saturates to a uniform high output intensity state.

A useful insight about the origin of the LS observed can be gained from the observation of Fig. 3. Fig. 3(a) shows the homogeneous steady state (HSS) characteristic of the system φ_0 vs αI_0 , together with the amplitudes of the localized and delocalized structures found in numerical simulations. In Fig. 3(b) it is shown the instability region of the homogeneous steady state.

In the rest of the paper we mostly discuss numerical results; hence it is convenient to refer to the adimensional parameter αI_0 as the pump, rather than to the intensity I_0 in physical units. In the conditions of the experiments here reported, $\alpha \simeq 18 cm^2/mW$.

The lower branch of the HSS destabilizes at $\alpha I_0 \simeq 28$, for a critical wavenumber $q_{c1} \simeq 0.71$. The critical point is better visible in the inset of fig. 3b, showing an enlarged portion of the stability balloon. The bifurcation from this point is strongly subcritical, and results in the formation of hexagons. The upper branch loses stability at $\alpha I_0 \simeq 20$, $q_{c2} \simeq 1.15$, with another subcritical bifurcation leading to the appearance of honeycomb patterns.

Our simulations show that both the hexagons and the honeycombs are unstable within most of their existence region. Indeed, hexagons typically decay toward a collection of spatially well separated round LS; honeycombs are instead destabilized either towards a collection of triangular LS, or towards a situation of developed space-time chaos, depending on the value of αI_0 . In order to stabilize the periodic patterns and be able to track their amplitudes, we introduced a filter in Fourier space allowing only for the existence of the six fundamental modes needed to create hexagons and honeycombs, plus all their harmonic combination up to the cutoff frequency fixed at 3.7. In this way we obtain the amplitudes for the delocalized patterns shown in Fig. 3a.

In the presence of the strongly subcritical patterns here observed, localized structures can be formed in the parameter range where an homogeneous stable steady state coexists, or is not far from, a patterned state [24]. These patterned states can be either stable or unstable for the parameter values at which LS exist. In the latter case, LS can be interpreted as residuals of some delocalized pattern that has lost its stability.

In our case, the superposition of the round LS and of the hexagon amplitudes seen in Fig. 3a clearly indicates the relation between the localized and delocalized structure. As for the relation between triangular LS and honeycombs, the results is less obvious from the data of Fig. 3a. We conjecture however that such a connection

exists also in this case. Our conjecture is based both on the general argument which describes the LS as local connections between a homogeneous and a patterned state; and, with specific reference to our case, on the triangular symmetry which is common to the localized structures and to the neighborhoods of local maxima in an honeycomb lattice.

We remind that the role of an honeycomb pattern in giving rise to cavity solitons has been already pointed out in [17], for a model of semiconductor optical resonator. In that case, contrary to ours, dark solitons are formed by a dip connecting a stable bright state and a local minimum of the pattern.

We concentrated our quantitative experimental investigations on the dependence of the phenomena observed on the pump intensity, while the other parameters were kept fixed. Let us now discuss how the other parameters affect the scenario. An exhaustive investigation of these dependencies is a demanding task, which we do not face at the moment. We will here limit ourselves to report about single parameter variations, with other parameters kept fixed at the values used above.

The major effect of a decrease of the system bandwidth q_B is a narrowing of the stability range for both solitons; the effect is more marked for triangular solitons than for round LS. As a consequence, small values of q_B lead to small ranges of soliton bistability. If q_B is set to values higher than $\simeq 4$, no substantial modifications occur with respect to the situation described above.

The combined role of diffusion and diffraction is expressed by the adimensional parameter $\sigma \equiv (2(l_d)^2 k_0/l)^{1/2}$, giving the ratio of the diffusion to diffraction parameter. The quantity σ can be viewed as an adimensional diffusion length. We are not in condition to have large excursion of σ in the experiment. The numerics show that an increase of σ with respect to the value used above leads to a shrinking of the stability range for both the round LS and the TS. The tendency is more marked for the triangular solitons, which have a stronger content of high frequency components.

The open loop phase φ_0 and the weights B and 1-B of the feedback fields tune the S shape of the homogeneous steady state solution, and modify the location and critical wavenumbers of the modulational instabilities affecting the lower and upper branches. For the value of B used above, bistability of LS is observed for $-0.4 \lesssim \varphi_0 \lesssim 0.1$. If φ_0 is kept fixed at 0, the two kinds of LS are bistable at $0.3 \lesssim B \lesssim 0.5$.

The saturation phase φ_{sat} turns out also to be a very important parameter. We refer also in this case to numerical results, since the saturation parameter can be little varied in the experiment. If φ_{sat} is lowered with respect to the value used above ($\varphi_{sat} = 5$), the stability range of TS moves to higher pump intensities, and these structures are no more observed when $\varphi_{sat} \lesssim 3.5$. If φ_{sat} is increased, triangular solitons continue to exist as well

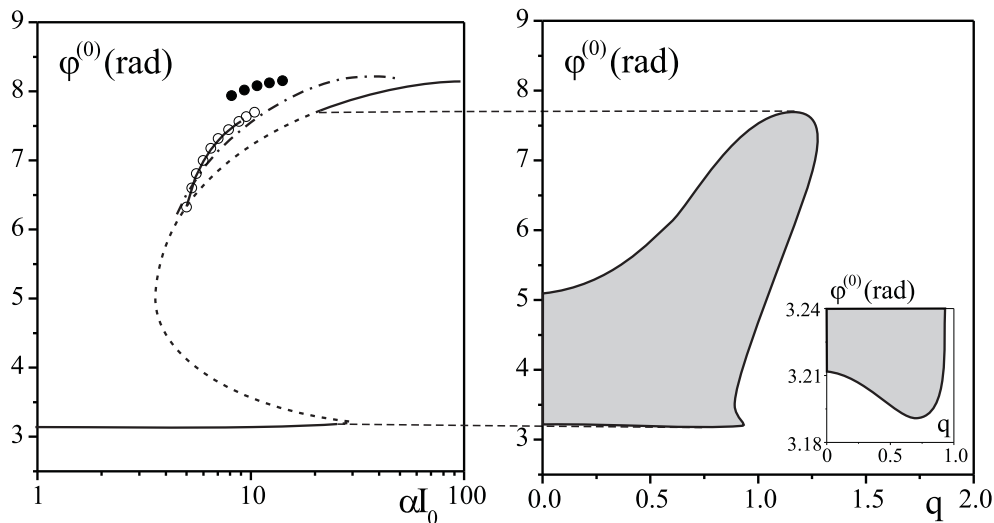


FIG. 3: Homogeneous steady state and its stability, together with localized and delocalized structure amplitude. For the values of parameters used, see text. In (a): Continuous line: homogeneous solution, stable parts, and hexagons bifurcating at the lower critical point ($q = 0.71$); dashed line: homogeneous solution, unstable parts; dash-dotted line: honeycombs bifurcating at the upper critical point ($q = 1.15$); empty circles: round localized structures; filled circles: triangular solitons.

as round LS up to $\varphi_{sat} = 18$. The range of bistability has a broad maximum at $\varphi_{sat} \simeq 6$, and then shrinks, until disappearing at $\varphi_{sat} \simeq 18$. Above this value, the round LS still exist; in correspondence of the branch formerly corresponding to triangular solitons, now only space-time chaotic delocalized patterns are observed.

In summary, we have reported the evidence of bistability between different localized structures in a non-linear optical interferometer. The observation of this phenomenon is completely new, and certainly more effort is required in order to obtain a full understanding of the sufficient and necessary conditions for its occurrence. Localized structure bistability occurs within a complex scenario of pattern forming events; still, it is clear that the phenomenon is robust with respect to parameter variations. This point, together with the generality of the mechanism lying at its basis, suggest that this phenomenon could be observed in systems of different nature.

This work has been partially supported by the Interuniversity Pole Program of the Belgian Government; by the Fonds National de la Recherche Scientifique; and by EU Contract HPRN-CT-2000-00158.

-
- [1] P. Umbanhowar, F. Melo and H. Swinney, *Nature* **382**, 793 (1996).
 [2] E. Moses, J. Fineberg and V. Steinberg, *Phys. Rev.* **A35**, 2757 (1987); K. Lerman, E. Bodenschatz, D.S. Cannell,

- and G. Ahlers, *Phys. Rev. Lett.* **70**, 3572 (1993).
 [3] M. Dennin, G. Ahlers, and D.S. Cannell, *Phys. Rev. Lett.* **77**, 2475 (1996)
 [4] H. H. Rotermund, S. Jakubith, A. Von Oertzen and G. Ertl, *Phys. Rev. Lett.* **66**, 3083 (1991); K.L. Lee, W.D. McCormick, Q. Ouyang and H. Swinney, *Science* **261**, 192 (1993).
 [5] For a comprehensive review, see e.g. Y.S. Kivshar and G.P. Agarwal, *Optical Solitons: from fibers to photonic crystals*, Academic Press (2003).
 [6] See e.g. *Feature section on cavity solitons*, *IEEE Journal of Quantum Electronics* 2003, **39**, n. 2 (2003).
 [7] M. Tlidi, P. Mandel and R. Lefever, *Phys. Rev. Lett.* **73**, 640 (1994).
 [8] W.J. Firth and A.J. Scroggie., *Phys. Rev. Lett.* **76**, 1623 (1996).
 [9] M. Saffman, D. Montgomery and D. Z. Anderson, *Opt. Lett.* **19**, 518 (1994).
 [10] A. Schreiber, B. Thuering, M. Kreuzer and T. Tschudi, *Opt. Comm.* **136**, 415 (1997).
 [11] P.L. Ramazza, S. Ducci, S. Boccaletti and F.T. Arecchi, *Journal of Optics B: Quantum and Semiclassical Optics* **2**, 399 (2000).
 [12] V.B. Taranenko, I. Ganne, R.J. Kuszelewicz and C.O. Weiss, *Phys. Rev. A* **61** 063818 (2000).
 [13] S. Barland et al., *Nature* **419**, 699 (2002).
 [14] A.E. Kaplan, *Phys. Rev. Lett.* **55**, 1291 (1985); R.H. Enns, S.S. Rangnekar and A.E. Kaplan, *Phys. Rev.* **A36**, 1270 (1987).
 [15] S. Gatz and J. Herrmann, *Journal of Opt. Soc. Am.* **B8**, 2296 (1991); W. Krolikowski and B. Luther-Davies, *Opt. Lett.* **17**, 1414 (1992).
 [16] G. Kozyreff, S.J. Chapman and M. Tlidi, *Phys. Rev.* **E68**, 015201 (2003).
 [17] D. Michaelis, U. Peschel and F. Lederer, *Phys. Rev.* **A56**, R3366 (1997).

- [18] J. McSloy, W.J. Firth, G.K. Harkness and G.L. Oppo, Phys. Rev. **E66**, 46606 (2002)
- [19] R. Neubecker, G.L. Oppo, B. Thuering and T. Tschudi, Phys. Rev. **A52**, 791 (1995).
- [20] S. Akhmanov, M.A. Vorontsov and V.Y. Ivanov, JETP Lett. **47**, 707 (1988).
- [21] G. D'Alessandro and W.J. Firth, Phys. Rev. Lett. **66**, 2597 (1991).
- [22] E. Benkler, M. Kreuzer, R. Neubecker and T. Tschudi, Phys. Rev. Lett. **84**, 879 (2000).
- [23] S. Rankin, E. Yao, and F. Papoff Phys. Rev. **A68**, 013821 (2003)
- [24] H. Riecke, "Localized structures in Pattern-Forming Systems" in *Pattern Formation in Continuous and Coupled Systems*, ed. by M. Golubitsky, D. Luss and S. Strogatz (IMA Volume 115, Springer, 1999), p. 215.
- [25] Ramazza P.L., Boccaletti S., Bortolozzo U. and Arecchi F.T., 2003 Chaos **13**, 335.
- [26] D. Michaelis, U. Peschel, C. Etrich and F. Lederer, IEEE journal of Quant. El. **39**, 255 (2003); S.V. Fedorov, N.N. Rosanov, A.N. Shatsev, N.A. Veretenov and A.G. Vladimirov, *ibidem*.
- [27] Ramazza P.L., Boccaletti S., Bortolozzo U., Ducci S., Benkler E. and Arecchi F.T., 2002 Phys. Rev. **E65**, 066204.